The natural transparency and piezoelectric response of the *Greta oto* butterfly wing

Valerie R. Binetti, Jessica D. Schiffman, Oren D. Leaffer, Jonathan E. Spanier and Caroline L. Schauer*

Received 12th November 2008, Accepted 30th January 2009
First published as an Advance Article on the web 12th February 2009
DOI: 10.1039/b820205b

The *Greta oto*, or the "glasswing butterfly", is a member of the Ithomiini tribe. Although rare among lepidopteran, the *G. oto*'s wings are naturally transparent. To understand the material properties of natural transparency, the various structures on the surface of the wings, both the transparent and brown "veins" and wing parameter regions were studied using scanning electron microscopy (SEM), transmission electron microscopy (TEM), reflectance spectrometry, transmission spectrometry and scanning probe microscopy (SPM) in order to investigate their local structure, periodic character, and electromechanical response. Nanosized protuberances in a highly ordered array were found on the surface of the transparent part similar to that of the "corneal nipple array" found in other insects as an antireflective device.

Introduction

Despite the importance of transparency in nature, it is not a well-understood phenomenon.[1] To be transparent, the organism or tissues must neither absorb nor scatter light, with the primary barrier to transparency being light scattering. To avoid light scattering, the organism must consist of a nonabsorbing species with a homogeneous refractive index. Because biological and chemical compounds found in most species have varying refractive indices, which closely correlate to density, the true basis for transparency must be due to the structurally organized features.

While most Arthropoda that use transparency as a successful camouflage live deep in the ocean, there are a few exceptions such as the wings of certain ithomiid butterflies, satyrid and sphingid moths[2] and the larvae of certain freshwater insects.[1] The *Greta oto*, (Fig. 1) or the "glasswing butterfly", is a member of the Ithomiini tribe and one of the Arthropoda exceptions that has transparent wings.

It is postulated that the surface of a transparent butterfly wing is covered with submicroscopic protrusions, which do not scatter light. The index of refraction is gradually changed over the protrusions from an index matching of air to an index matching of the material within the wing. This changing index of refraction is similar to what is observed in certain "moth eye" surfaces of butterflies[3,4] that reduce visibility and "corneal nipple arrays" found in the structural units of compound eyes of certain insects, which act as an antireflective device.[5–8] Similar to what is observed in glass, there must be highly destructive interference present and no light scattering. While much of the terrestrial transparency theory applies to extracellular tissues, it cannot adequately predict intercellular optical transparency.

Fig. 1 Photograph of a *Greta oto* butterfly. The *G. oto* in this photograph has a wingspan of roughly 47 mm.

The various scale types and other structural features on the surface of the *G. oto* wing were determined with the use of scanning probe microscopy (SPM), scanning electron microscopy (SEM) and transmission electron microscopy (TEM), including also an analysis of the spatial periodicity of the

Department of Materials Science and Engineering, Drexel University, Philadelphia, PA, USA. E-mail: cschauer@coe.drexel.edu

Insight, innovation, integration

This work provides biological insight into the role of natural transparency in the *G. oto* utilizing optical, piezoelectric, structural and chemical analysis. Because biological and chemical compounds have varying refractive indices, the true basis for transparency must be due to the structurally organized features. While structural coloration is commonly used for predatory behavior or mating, natural transparency has a unique role for the glasswing butterfly.

protuberances on the wing. The chemical and crystalline nature of the *G. oto* wing was also determined using Fourier transform infrared spectroscopy (FTIR) and X-ray diffraction (XRD) and compared to two butterflies within the same Nymphalidae family.

Solid state materials that lack a center of inversion symmetry—whether synthetic or naturally occurring—satisfy a requirement for piezoelectricity, the property that describes the coupling of an applied mechanical stress to an induced electric displacement. It has been proposed that piezoelectricity and its conjugate effect, converse piezoelectricity (in which applied fields result in induced strain), may play a role in the growth, function (and possibly evolution) of biological and physiological systems.[9] Piezoresponse force microscopy (PFM),[10] a member of a family of SPM techniques, is used in conjunction with topographic height for mapping the local piezoelectric properties of materials. In PFM, the topography of a sample is collected, typically in a net repulsive force interaction mode. Vector PFM[11] (VPFM) is a variation of PFM in which the local magnitude of piezoelectric response and orientation of entities (*e.g.* grains, ferroelectric domains, molecules) producing the polar response can be ascertained. Recently, Kalinin *et al.*[12] used these techniques to obtain correlated local maps of topography, piezoelectric response and dipolar orientation, and modulus of a number of biomaterials, including *Vanessa virginiensis* butterfly, in addition to a human tooth. In this work, topographic SPM, PFM and VPFM were used, with SEM and TEM, to investigate the apparent structure–property relationships of the naturally transparent *G. oto* wing at the nanoscale.

Investigation into tropical butterflies' patterns and flight speed[13] have led to the understanding of mimicking as a defense against rufous-tailed jacamars, the *G. oto* being sight rejected by these birds. *G. oto*'s defense against predators has been investigated with respect to its pupae attachment[14] and the food it ingests[15] (larval prey chemistry[16]) which is also used by other Ithomiini for defense.[17] While structural coloration is commonly used for predatory behavior or mating, natural transparency has a unique role for the glasswing butterfly. The range of transparency with respect to typical predators will give rise to a better understanding as to the use of transparency for defense.

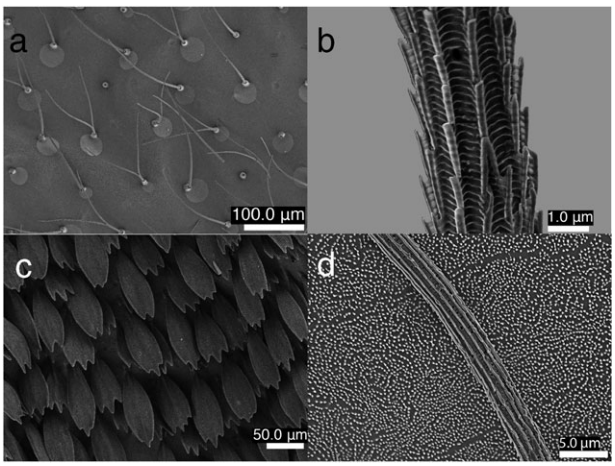

Fig. 2 SEM images showing three distinct patterns on the wing of the *G. oto*. Image **a** shows the piliform scales found on the transparent part of the wing, **b** shows a detailed image of a piliform scale, **c** shows the flat scales on the brown colored part of the wing and **d** shows a piliform scale and the underlying pattern beneath the piliform scales on the transparent part of the wing.

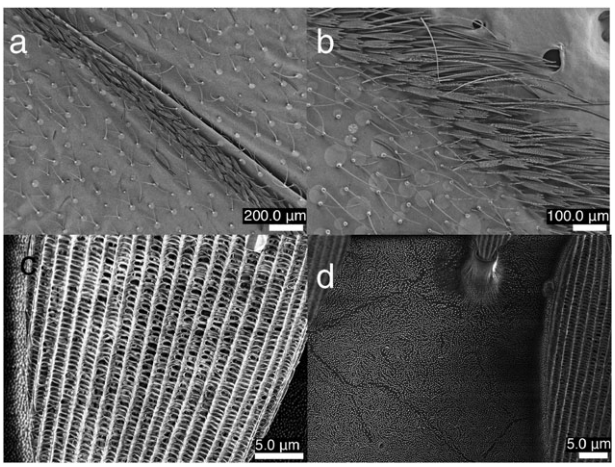

Fig. 3 SEM images showing scales and patterns on the surface of the *G. oto* wing: **a** a combination of flat and piliform scales along a "vein" on the wing, **b** a combination of flat and piliform scales at the edge of the wing, **c** structure of the heart-shaped flat scale and **d** oval shaped scales and the underlying pattern beneath the scales.

Results and discussion

Piliform scales

Piliform scales[18] or bristles[19] are commonly referred to as "hairs";[20] they are high aspect ratio features on the surface of the butterfly wings (Fig. 2a, b and d) and could possibly have three distinct patterns: *Morpho*-, *Urania*- and undifferentiated. Piliform scales on species that exhibit *Morpho* (flute)-type scales, such as the *Spindasis syama*, *Spindasis nipalicus*, *Rapala rhoecus* and *Artipe eryx*, do not show *Morpho*-like nor *Urania* (pepper-pot)-like structure and are therefore undifferentiated.[20] Structurally colored *Polyommatus coridon* and *Tomares ballus* have *Urania*-type piliform scales, in addition to flat scales that also exhibit the *Urania*-type structure.[20] The *G. oto* is sparsely clothed in piliform scales on the transparent part of the wing (Fig. 2a); these piliform scales are undifferentiated. The brown colored "veins" of the wing of the *G. oto* show an intermixing of piliform and flat scales (Fig. 3a); this intermixing is also present on the edge of the wing (Fig. 3b).

Flat scales

In addition to the piliform scales, the *G. oto* has flat scales on the "veins" and along the outer perimeter of the wing. Flat scales are found in three distinct patterns: *Morpho*-, *Urania*- and undifferentiated. These flat scales differ in shape depending on where they are located on the wing. These scales are either "heart-shaped" (Fig. 3c), oval (Fig. 3d), "fan" or of rounded shape at the base and tooth shaped at the tip of the

scale (Fig. 2c). All of the various shaped flat scales appear to be undifferentiated. These flat scales give rise to the brown coloring on the "veins" and the outer perimeter of the *G. oto* wing; the white colored sections on the upper wings are made up of tooth shaped scales (Fig. 2c).

Underlying pattern

On the *G. oto* wing, between the flat (Fig. 3d) and piliform (Fig. 2d) scales, there is an underlying hexagonally packed pattern of triangular shaped protuberances, which are roughly 320 nm in diameter and 80 nm in height. This hexagonal pattern is similar to that found on the Hawkmoth, *Cephonodes hylas*, by Yoshida *et al.*[21] and in the "corneal nipple arrays" studied by Bernhard and Miller.[22]

Cross-sectional structure

TEM images of the *M. rhetenor* and the *M. didus* reveal the discretely configured multi-layered arrays which occur vertically throughout their wings.[23] The distinct pattern observed correlates to the strong structural color observed in these wings. Therefore, the cross-sectional image of the *G. oto* was investigated to differentiate the internal pattern of the wing, as well as to calculate the wing's thickness. The TEM image in Fig. 4 is of a vertical slice of the transparent region of the wing. The vertical slice highlights the thickness of the wing and size and spatial nature of the protuberances.

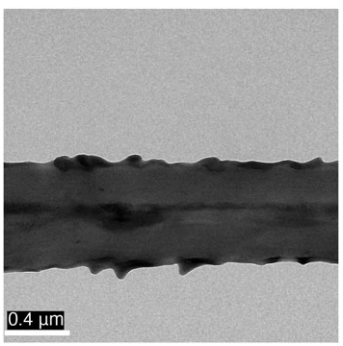

Fig. 4 TEM image showing a cross section of the transparent region of the *G. oto* wing. The size and spatial nature of the protuberances are highlighted, as well as the thickness of the wing.

Fourier transform infrared spectroscopy and X-ray diffraction

FTIR of the *G. oto* is similar to that of another butterfly within the Ithomiini tribe, the *Godyris duillia*, and to the *Vanessa cardui*, a member of the Nymphalini tribe (Fig. 5a). Since butterfly wings predominantly consist of α-chitin plus proteins and possibly pyrrolizidine alkaloids (a main component of the *G. oto*'s food[24] and used to defend against predators[17]), the *G. oto*, *G. duillia* and *V. cardui*[25] have similar key FTIR peaks, though the intensity of these peaks varies between species. Key peaks are found at 3450 cm^{-1} for OH stretching; 3270 cm^{-1} for the axial deformation of the NH group; 2850 cm^{-1} for CH stretching; and 1550 cm^{-1} for the amide II peak. The key difference between the *G. oto* and *V. cardui* is that the 1631 cm^{-1} absorbance peak, the amide II peak from the amine functionality, is pronounced in the *G. oto* but is only a shoulder in the *V. cardui*. Traditional bulk α-chitin alcohol region is stronger in pure bulk α-chitin than in the *G. oto* spectrum, while the *G. oto* amide region is more pronounced, due to the contributions of the proteins, than in the pure bulk α-chitin. The shoulder peaks at 1720 cm^{-1} and 1220 cm^{-1} indicate the presence of proteins, as well as possibly pyrrolizidine alkaloids in the wing.[26]

The XRD spectra of the bulk α-chitin, *G. oto*, *G. duillia* and *V. cardui* were measured and compared (Fig. 5b). The *G. oto* and *G. duillia* show similar XRD peaks to that of *V. cardui*, a brown and orange colored butterfly that like the *G. oto* and *G. duillia* is a member of the order Lepidoptera and family Nymphalidae but differs in that it is a member of the Nymphalini tribe. All three butterflies examined have similar XRD spectra compared to bulk α-chitin, with the sharp peak centered around $2\theta = 17^\circ$ indicative of the (040)/(110) diffraction plane, as well as a peak at $2\theta = 19^\circ$, the (120) peak.[25]

Reflectance spectrometry

The reflectance and transmission (Fig. 6) of the transparent portion of the unprocessed *G. oto* wing were measured from the middle ultra-violet (UV) through the near infrared, over

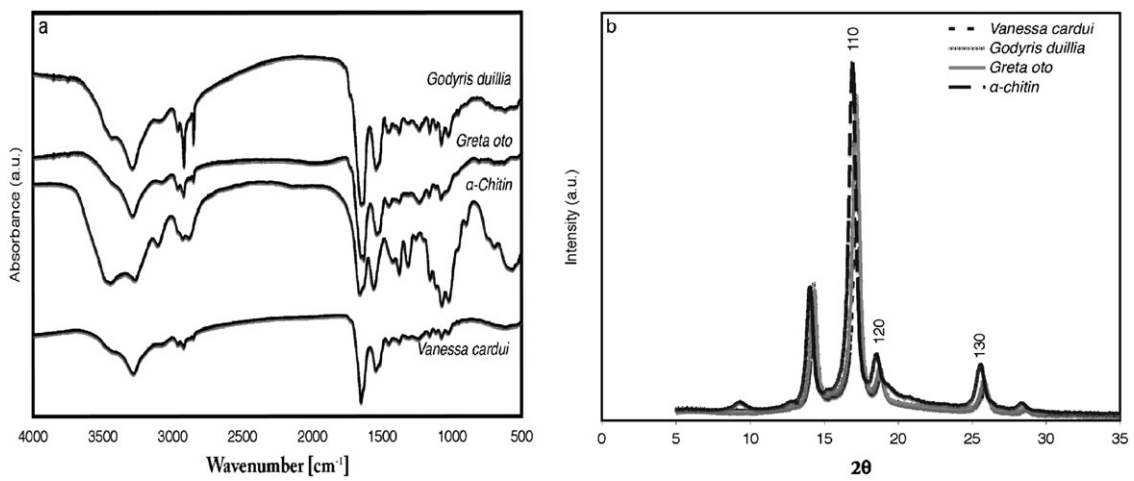

Fig. 5 FTIR (a) and XRD (b) spectra of the entire wing of *G. duillia*, *G. oto* and *V. cardui* with α-chitin for reference.

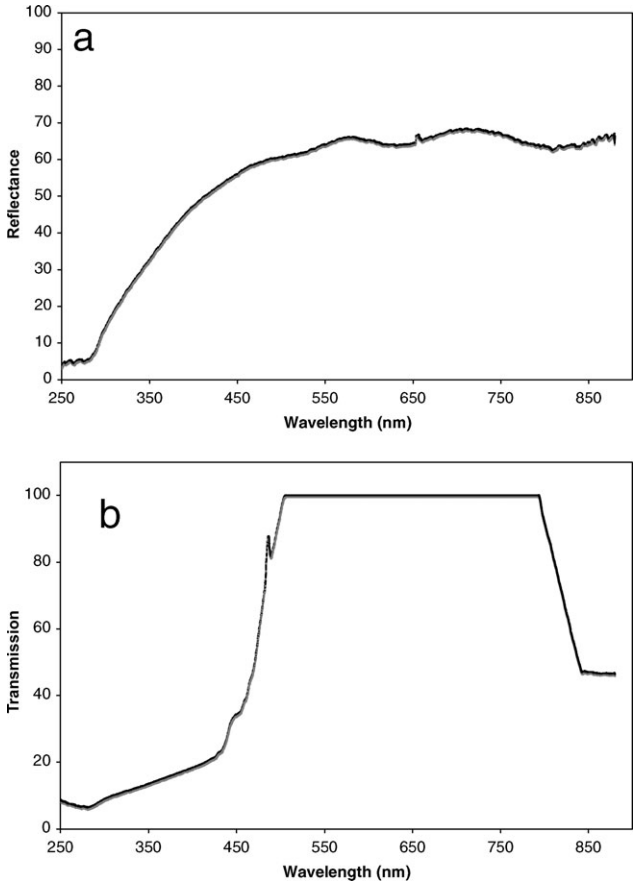

Fig. 6 Reflectance and transmission spectra of transparent area of *G. oto* wing over the wavelength range of 250–900 nm: **a** is the reflectance plot taken of the wing placed on a polished silicon wafer, and **b** is the transmission plot.

the wavelength range of 250 to 900 nm. Fig. 6a shows the reflectance spectrum of the wing placed on a polished silicon wafer. The measured light was 180° back reflected from the sample. Fig. 6b shows the transmission spectrum, measured through the transparent part of the *G. oto* wing, has 100% transmission from 500 to 800 nm, from green to red in the color spectrum.

Scanning probe microscopy

SPM was performed on transparent regions of the wing of *G. oto* in intermittent contact, and alternately, in a net repulsive-force (contact) mode. Shown in Fig. 7a and 7b are topographic height maps of 10×10 μm^2 and 4×4 μm^2 areas in which the morphological organization of the chitin and protein-based nano-crystallites is clearly discerned (Fig. 7d), as well as the structure within the piliform scales (inset of 7b).

The topographic scans indicate three basic features at the nano-scale: quasi-periodic close-packed structures (*i*) without (Fig. 7a), and (*ii*) with (Fig. 7b) long spatial-wavelength curvature in the periodic organization of the chitin and protein-based nano-crystallites, and (*iii*) linear/lamellar structures (inset of Fig. 7c, 300×300 nm^2). Locally, as seen in Fig. 7a–c, the organization of the nano-crystallites possesses quasi-periodicity with pseudo-monoclinic symmetry and a spatial wavelength on the order of ~200 nm, as confirmed in a two-dimensional Fourier transform of the topographic height of Fig. 7c (inset of Fig. 7c, scale $\sim 60 \times 60$ m^{-2}), in which six peaks in reciprocal space are located around $k_x = k_y = 0$, and possess elongated character in k_y, consistent with the real-space elongation of the unit cell structure. Though hexagonal periodic character has been observed on the hawkmoth, the protuberances seen in the transparent regions of *G. oto* appear to be unique among all species for which information on the transparent regions is available, in that each protuberance is triangular, rather than semicircular, and their organization possesses pseudo-monoclinic symmetry. In light of this quasi-periodicity, the remarkable apparent optical transparency throughout much of the visible spectrum of a significant portion of the wing of *G. oto*—a feature that is distinct from most other species found in similar habitats in the same geographic region and elsewhere—suggests an intriguing and non-trivial relationship between hierarchical structure and macroscopic optical response that merits further investigation.

The local polar molecular character of the *G. oto* wing was probed by PFM.[10] A variation of PFM, VPFM,[12] has been applied to a variety of inorganic thin-film piezoelectric materials, and increasingly, in biomaterials.[9] VPFM permits a semi-quantitative description of the local orientation of the polar character of the material under study by resolving the normal and lateral components of the local electromechanical response, and rendering this response using a circular wheel color map. Here, the normal and one of the in-plane components of the local piezoelectric response were collected simultaneously during the collection of topographic height to eliminate possible artifacts that are associated with drift. For the PFM measurements, a small sinusoidal perturbing ac voltage (5 V, 7 kHz) was applied to the cantilever tip with respect to the electrically grounded substrate, resulting in an electric field-induced local mechanical response owing to the converse piezoelectric effect. The PFM data channels were collected with the aid of a lock-in amplifier (Stanford SRS830). The output signal of the lock-in amplifier is displayed as a spatial map that allows correlation of topographic height with local piezoelectric response. Shown in Fig. 7d is the superposition of the processed VPFM signal on the height data shown in Fig. 7c.

Analysis[12] of the spatial character of the local VPFM signal permits a semi-quantitative interpretation of the local polar orientation of the chitin, and its correlation with hierarchical organization found in the *G. oto* wing. Within a single protuberance, a distribution of orientations is observed, as seen in Fig. 7d. The orientations relate to the organization of chitin and protein within the *G. oto* protuberances.

Conclusions

As in Kalinin's work with the *Vanessa virginiensis* butterfly,[12] the VPFM map in Fig. 7d shows piezoelectric properties that are position-dependent; the protuberances and other features on the surface of the *G. oto* wing give uniform responses. Local polar character identified using VPFM and other techniques

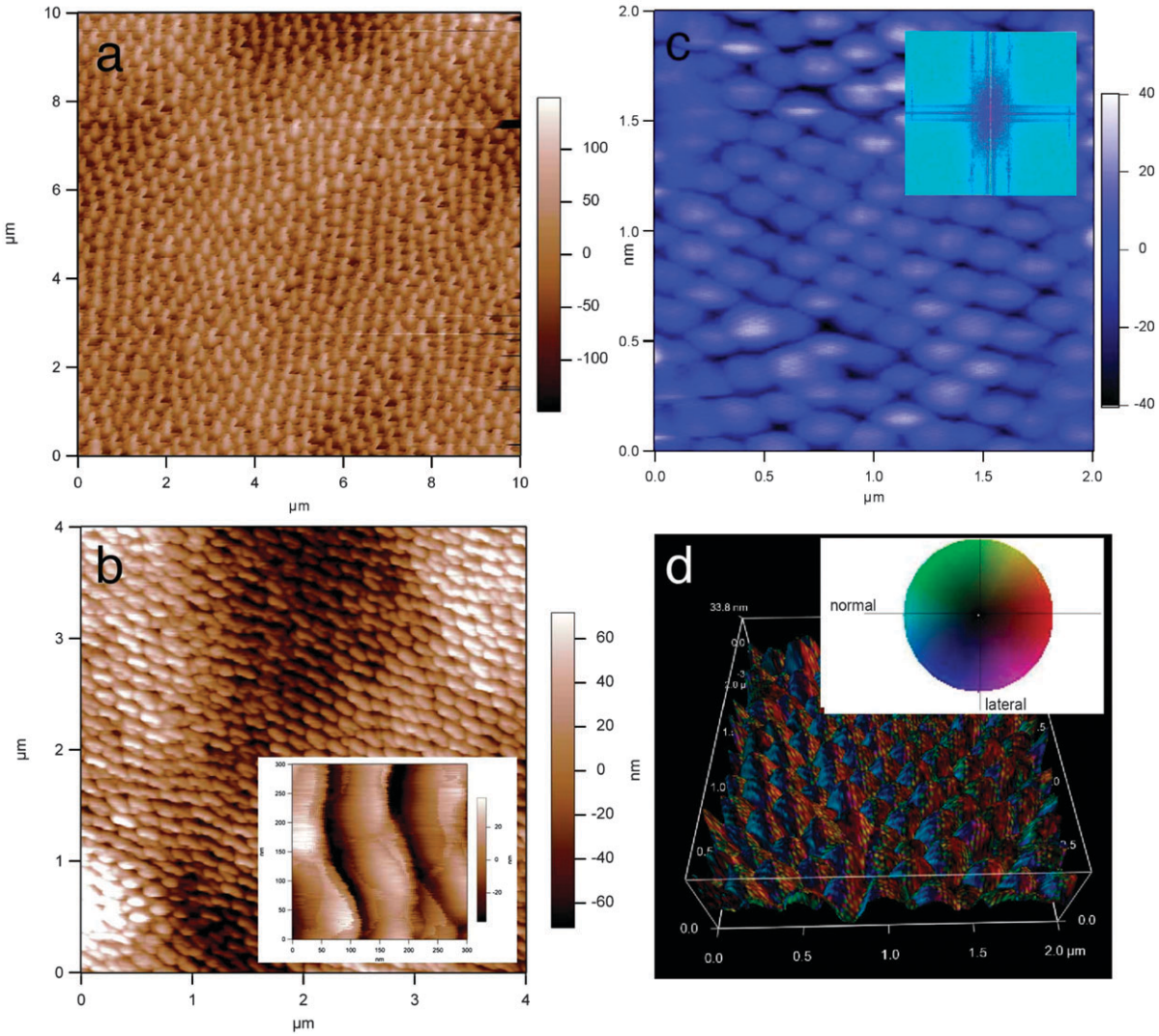

Fig. 7 Scanning probe microscopy of *G. oto*: **a**, 10 μm^2 and **b**, 4 μm^2 topographic height images, demonstrating different organization and character of structural protuberances, including both structures shown in Fig. 1d and structure within piliform scales (inset of **b**); **c**, 2 μm^2 topographic height image, along with a two-dimensional Fourier transformation, full-scale range 60 × 60 m^{-2} (inset), revealing pseudo-monoclinic symmetry, and **d**, superposition of the vector piezoresponse force microscopy signal on the topographic image shown in **c**, revealing local variations in the magnitude and direction of the converse piezoelectric response.

can add value towards elucidating function[5,27] and remarkable optical properties.

The hexagonal packing of the *G. oto* protuberances is indicative of structurally derived natural transparency. Even though the protuberances are shaped differently than those observed for the transparent region of the hawkmoth, pyramidal rather than circular, the two-dimensional packing arrangement appears to be conserved. Unlike what has been seen in other structurally colored Nymphalidae examples, the cross-sectional area did not possess structural details throughout the *G. oto* wing. Therefore, the hexagonal packing is the key feature for natural terrestrial transparency.

The main predator for Ithomiini butterflies are various birds, which are known to have keen eyesight,[28] due to their bright plumage and ability to distinguish slight movements. With *G. oto*'s 100% transmission of light through the wing in the visible (green to red) wavelengths for camouflage, the *G. oto* is well adapted for camouflage.

Experimental

All butterfly samples were acquired dried and all experiments were performed in compliance with the relevant laws and institutional guidelines.

Fourier transform infrared spectroscopy (FTIR)

FTIR spectra were collected using a Varian Excalibur FTS-3000 in transmission mode. The *G. oto* wing specimens were used directly, unprocessed and in one piece. Spectra were taken in the spectral range of 4000–500 cm^{-1} by accumulation of 64 scans and with a resolution of 4 cm^{-1}.

Reflectance spectrometry

Reflectance spectrometry was done with an Ocean Optics Inc. USB2000 miniature fiber optic spectrometer with DH-2000 deuterium tungsten halogen light sources. Reflectance of the wing was measured on a highly reflective surface, a highly

polished silicon wafer. The wafer was used to calibrate a baseline and then the wing was placed on top of the wafer to measure the reflectance. Transmission of the wing was measured through the wing in air.

Scanning electron microscopy (SEM)

Scanning electron microscopy was conducted with a Zeiss Supra 50/VP field emission scanning electron microscope (FESEM). The wing was coated with platinum-palladium using a Denton vacuum desk II sputtering machine.

Scanning probe microscopy (SPM)

For SPM analysis, a portion of an unfolded wing of *Greta oto* was placed on a wet conductive silver-paste-coated borosilicate glass slide ("substrate"), and probed with a Ti–Pt-coated SPM cantilever (Olympus AC240TM, $k \sim 2$ N m^{-1}, $f \approx 70$ kHz) using a scanning probe microscope (Asylum Research MFP-3D, Santa Barbara CA) within a darkened acoustic enclosure at ambient temperature and humidity.

Transmission electron microscopy (TEM)

Transmission electron microscopy was performed on a JEM-2000 FX, 200 kV, LaB_6 gun TEM. The *Greta oto* wing was sectioned at 45°; this section was mounted in EPOFIX resin, mixed in an 8 : 1 mix ratio. Thin (70 nm) sections of the butterfly were cut with a Leice EM UC6 ultramicrotome using a DiATOME 35° diamond knife, floated on the water surface, and then collected on a TEM copper grid.

X-ray diffraction (XRD)

X-ray diffraction was conducted using a Siemens D500 X-ray powder diffractometer. The wing was attached to a glass microscope slide with double sided tape.

Acknowledgements

The authors would like to thank Michael Birnkrant and John Sampson for TEM discussions and help. VRB, ODL and JDS would like to thank Graduate Assistance in Areas of National Need-DREAM (P200A060117), which is funded by the Department of Education's office of Postsecondary Education for funding. JES acknowledges support from the U. S. Army Research Office (W911NF-08-1-0067). CLS acknowledges support from NSF (CMMI 0804543).

References

1 S. Johnsen, *Biol. Bull.*, 2001, 301–318.
2 A. Yoshida, M. Motoyama, A. Kosaku and K. Miyamoto, *Zool. Sci.*, 1996, 13.
3 R. Singer and A. A. Cocucci, *Bot. Acta*, 1997, **110**, 328–337.
4 D. G. Stavenga, S. Foletti, G. Palasantzas and K. Arikawa, *Proc. R. Soc. London, Ser. B*, 2006, **273**(1587), 661–667.
5 G. S. Watson and J. A. Watson, *Appl. Surf. Sci.*, 2004, **235**, 139–144.
6 W. H. Miller, G. D. Bernard and J. L. Allen, *Science*, 1968, **162**, 760–767.
7 C. G. Bernhard, G. Gemne and J. Sällström, *J. Comp. Physiol., A*, 1970, **67**, 1–25.
8 A. R. Parker, Z. Hegedus and R. A. Watts, *Proc. R. Soc. London, Ser. B*, 1998, **265**, 811–815.
9 S. V. Kalinin, B. J. Rodriguez, S. Jesse, T. Thundat and A. Gruverman, *Appl. Phys. Lett.*, 2005, **87**, 3.
10 A. Gruverman, O. Auciello and H. Tokumoto, *Annu. Rev. Mater. Sci.*, 1998, **28**, 101–123.
11 S. V. Kalinin, B. J. Rodriguez, S. Jesse, J. Shin, A. P. Baddorf, P. Gupta, H. Jain, D. B. Williams and A. Gruverman, *Microsc. Microanal.*, 2006, **12**, 206–220.
12 S. Kalinin, B. Rodriguez, J. Shin, S. Jesse, V. Grichko, T. Thundat, A. Baddorf and A. Gruverman, *Ultramicroscopy*, 2006, **106**, 334–340.
13 P. Chai, *Biol. J. Linn. Soc.*, 1986, **29**, 161–189.
14 A. Ingram and A. Parker, *Entomol. Sci.*, 2006, **9**, 109–120.
15 S. Hall, *Tropical Lepidoptera*, 2008, **7**, 161–165.
16 L. A. Dyer, *Ecology*, 1995, **76**, 1483–1496.
17 K. Brown, *Nature*, 1984, **309**, 707–709.
18 J. C. Downey and A. C. Allyn, *Bull. Allyn Mus.*, 1975, **31**, 1–32.
19 H. Ghiradella, *Hairs, Bristles and Scales*, Wiley-Liss, New York, 1998.
20 R. J. D. Tilley and J. N. Eliot, *Trans. Lepidopterol. Soc. Jpn.*, 2002, **53**, 153–180.
21 A. Yoshida, M. Motoyama, A. Kosaku and K. Miyamoto, *Zool. Sci.*, 1997, **14**, 737–741.
22 C. G. Bernhard and W. H. Miller, *Acta Physiol. Scand.*, 1962, 385–386.
23 P. Vukusic and J. Sambles, *Nature*, 2003, **424**, 852–855.
24 S. Hall, *Tropical Lepidoptera*, 1996, **7**, 161–165.
25 J. D. Schiffman and C. L. Schauer, *Mater. Sci. Eng., C*, 2009, **29**, DOI: 10.1016/j.msec.2008.11.006.
26 A. S. Prakash, T. N. Pereira, P. E. B. Reilly and A. A. Seawright, *Mutat. Res.*, 1999, **443**, 53–67.
27 G. S. Watson, S. Myhra, B. W. Cribb and J. A. Watson, *Biophys. J.*, 2008, **94**, 3352–3360.
28 N. S. Hart, *Prog. Retinal Eye Res.*, 2001, **20**, 675–703.